

Microscale Residual Strains in Monolayer Unidirectional Fiber Composites

Jay C. Hanan¹, Bjørn Clausen¹, Geoffrey A. Swift¹, Ersan Üstündag^{1,*}
Irene J. Beyerlein², Jonathan D. Almer³, Ulrich Lienert³, Dean R. Haeffner³

¹ Department of Materials Science, M/C 138-78, California Institute of Technology
Pasadena, CA 91125, USA;

² Theoretical Division, Los Alamos National Laboratory, Los Alamos, NM 87545, USA

³ Advanced Photon Source, Argonne National Laboratory, Argonne, IL 60439, USA

Keywords: Ti-6Al-4V, SiC, metal matrix composites, residual strains, plastic anisotropy, X-ray diffraction.

Abstract. Thermal residual stress is common in fiber reinforced metal matrix composites and significantly affects their mechanical properties. The calculation of these stresses typically assumes continuum mechanics holds. As the fiber diameter in most composites approaches the grain size of the matrix, the continuum assumption can become invalid. Since the mechanical properties depend on the residual strain state of the composite, it is therefore necessary to determine the residual strains using spatially resolved microscale measurements. In order to quantify these residual strains, X-ray diffraction of both the fiber and matrix was employed using a sampling volume less than the fiber diameter. Results were compared to macroscopic measurements including many fibers. The measurements were performed in transmission using high-energy synchrotron X-rays yielding strains representative of the entire thickness of the composite. Evolution of these residual strains after application of load was also investigated. Spatial variations in residual strains showed significant deviation from the macroscopically observed residual strains.

Introduction

Residual stress is one of the fundamental factors affecting composite strength, lifetime and fracture toughness, by helping or hindering the nucleation of damage (e.g., fiber breaks, interface debonding, and matrix plasticity). It is a sensitive variable that depends on fiber/matrix interface properties, constitutive behavior of matrix and fibers, geometric arrangement of fibers, fiber volume fraction and processing conditions. Considering the variation in these material and geometric properties, some variation in the residual stress is expected. In composites, the macroscopic stress-strain curves obtained by conventional means result from the co-deformation of the individual phases making it impossible to determine the phase specific *in-situ* constitutive behavior directly. Calculating residual stress from measured strain is further complicated since the *in-situ* mechanical properties of the constituents are significantly different from those of their monolithic forms [1,2]. Using X-ray microdiffraction, the phase specific *in-situ* residual and applied tensile strains in a model Ti-matrix / SiC-fiber composite were investigated at a resolution less than the fiber diameter. The grain size of the matrix approached the diameter of the fiber. Therefore, variation in the residual strains due to grain-to-grain interactions in the matrix was expected to influence the local fiber strains. Since the mechanical properties depend on the residual strain state of the composite, it was therefore necessary to determine the residual strains using spatially resolved microscale measurements. The diffraction data suggested that although the average strains reflected the results obtained through macroscopic measurements, significant local variations were also observed.

* Corresponding author; electronic mail: Ersan@caltech.edu.

Experimental Procedure

Sample Preparation. The studied composite system consisted of a single row of unidirectional SiC fibers (Textron SCS-6, 140 μm in diameter) in a Ti-6Al-4V matrix, prepared by a proprietary technique at 3M Corp. (St. Paul, MN 55144). The fibers were uniformly spaced with an average center-to-center distance of 240 μm . The measured fiber area fraction was 32%. The specimen dimensions were: thickness, $t = 0.20$ mm, gage length, $L = 26.00$ mm, and gage width, $W = 7.00$ mm. The composite was nominally damage free.

X-ray Diffraction Experiments. 25 keV X-rays (wavelength, $\lambda = 0.496$ Å) were employed at the 1-ID-C beam line (SRI-CAT, Sector 1), Advanced Photon Source (APS), Argonne National Laboratory. For this composite, 25 keV X-rays have an average transmitted beam intensity that is 58% of the incident beam intensity. Assuming an exponential decay in the transmitted intensity from the sample surface inward, the midpoint of the sampling volume was 91 μm from the surface facing the incoming X-ray beam. Therefore, these measurements were not confined to a thin surface layer but were representative of the entire thickness of the composite (200 μm).

To obtain the desired diffraction geometry, a four-circle goniometer was used in transmission mode. The diffraction vector was along the fiber axis, thus the diffraction patterns provided the longitudinal (or axial) strain in the plane of the composite. The diffraction intensity was collected with a NaI scintillator detector equipped with a Si (111) analyzer crystal. The X-ray beam size was defined by slits on the incident beam side. An internal standard Si powder (NIST, Standard Reference Material 640a) was attached to the specimen surface to minimize experimental errors.

The sample was scanned with a 2×2 mm² beam to obtain the average bulk residual strains and response of the composite to applied stress. These $\theta/2\theta$ scans were conducted over a range of $2\theta = 10^\circ$ to 24° . The data exhibited reflections from β -SiC, α -Ti, Si powder, and to a lesser extent β -Ti, which comprised a small fraction of the matrix. In order to allow Rietveld refinements [3], 0.007° steps in 2θ were used. The Rietveld analysis was performed using the GSAS package [4]. In addition, individual peaks were also fit using a Lorentzian peak profile.

As a comparison, a region of the composite was also scanned using a 90×90 μm^2 beam. This region was divided into 13 fiber and 9 neighboring matrix positions. At each fiber location, the SiC (220) peak was scanned; and at each matrix position, the α -Ti (10-2) peak was scanned.

A stress-free fiber reference was obtained by dissolving the matrix with 25% hydrofluoric acid. Similarly, a matrix reference was obtained by etching away a 0.1 mm layer of the composite. The remaining matrix easily separated from the fibers since the thermal residual stresses were relieved.

The composite was stressed in tension using a custom-built load frame. A strain gage was attached to measure the applied macroscopic strain at the surface in the longitudinal direction (parallel to fibers) while the applied load was logged by computer via a load cell.

Finite Element Modeling

To better understand the evolution of internal stresses/strains in the composite, a finite element model (FEM) was developed. This model assumed plane strain conditions because of the continuous fiber geometry. The planes perpendicular to the fiber direction ($z = \text{constant}$) were kept as planes. The plane parallel to the fiber where x was equal to half the fiber spacing was also kept planar to produce a continuous boundary condition for an infinite number of fibers. The surface of the composite (where $y = t/2$) was free to deform. The planes $x = 0$, $y = 0$, and $z = 0$ were general symmetry planes. The relative dimensions of the fiber and matrix regions in the model were adjusted to obtain a fiber area (and volume) fraction of 0.32 to correspond to the measured value.

The measured *initial* thermal residual strains (see Table 1: -1530 $\mu\epsilon$ for SiC and $+2200$ $\mu\epsilon$ for Ti, where $\mu\epsilon = 10^{-6}$ strain) were included in the calculation as they would be present in the composite before tensile loading. The material parameters for the matrix and the fibers were taken from refs. [5,6]. Specifically, the room temperature values of the elastic constants for the matrix were $E_m = 125$ GPa and $\nu_m = 0.31$, whereas those for the fibers were $E_f = 393$ GPa and $\nu_f = 0.25$ (both were assumed elastically isotropic) [5]. The variation of these elastic constants with

temperature was also included in the calculation in addition to the temperature-dependent values of coefficients of thermal expansion (CTEs) given in [5]. The fibers were assumed linear elastic and intact throughout the loading. Note that the tensile strength of the SCS-6 fibers is known to exceed 3 GPa [7]. The Ti-6Al-4V matrix was modeled as an elastic-plastic material with a yield strength of 725 MPa (where first deviation from linear elasticity occurs), an engineering yield strength ($\sigma_{0.2}$) of about 920 MPa and a linear strain-hardening coefficient of 1.63 GPa. These parameters were deduced from ref. [6] where the tensile behavior of the Ti-6Al-4V alloy was determined. Finally, the fiber/matrix interface was assumed intact at all times.

The FEM predicted no appreciable variation in the longitudinal elastic strain in either phase across the specimen thickness. This aided in the interpretation of the diffraction data, which represented the bulk average across the specimen thickness. Only a thin layer in the matrix around the fiber showed a decrease in elastic strain due to initiation of plastic deformation. The FEM predicted the plastic deformation in the matrix to start around 150 MPa applied composite stress. This occurred due to the three-dimensional stress state at the interface, i.e., the matrix had longitudinal and tangential tension and radial compression resulting in a large von Mises stress at the interface that exceeds the uniaxial yield strength (725 MPa). However, macroscopic plasticity was not detectable until about 600 MPa applied composite stress. Note that the tensile axial residual stress in the matrix (+350 MPa, see below) aids its early yielding.

Results and Discussion

This study yielded information about the evolution of residual stresses/strains in the composite under loading and the bulk *in-situ* mechanical behavior of Ti and SiC. Fig. 1 exhibits strain data as a function of tensile longitudinal stress during a loading/unloading cycle. Some of the data are also shown in Table 1. The *initial* residual strain data in Table 1 was collected with both a large X-ray beam (2x2 mm²) as well as a small one (90x90 μm²). The latter beam size was used at 13 different fiber and 9 matrix locations. These locations were away from the region where the macro data was collected (with the large beam). Significant scatter in the microscale strain data across these locations was observed. Before loading, the fibers exhibit an average longitudinal compression of -1530 με due to thermal residual strains. At the microscale, this value is -1790 με with a standard deviation of 190 με. The macro strain data is roughly within the standard deviation of the microscale data. The measurement error for all strains was about 100 με.

The fiber strains were based on measurements from only one reflection (the (220) of β-SiC which is a cubic phase). This resulted from the high texture and small grain size (about 50-100 nm) found in the fibers. Few SiC reflections were observed in the diffraction patterns, and among those, only (220) yielded good statistics. The literature values for this system confirm the thermal residual strains in the fibers shown here. Withers and Clarke [6] and Choo *et al.* [8] used neutron diffraction and quoted the same residual strain value for the SiC fibers in the longitudinal direction as that found in this work (the *macro* strain data). The former used the (220) reflection as well, but the latter performed Rietveld analysis on β-SiC. In addition, Rangaswamy *et al.* [5] obtained a similar value (about -1300 με) using the same reflection. In summary, the (220) reflection of β-SiC is representative of the internal stress/strain state of the fibers. As further confirmation, in Fig. 1, the strains along (220) follow closely the FEM predictions for the fibers.

Table 1. Residual strain evolution in the Ti-SiC composite.

	β -SiC (220)	α -Ti (Rietveld)	α -Ti (10-2)	α -Ti (11-0)
Initial (Thermal) Residual Strain ($\times 10^{-6}$)	-1530 (± 70) -1790 (± 190)*	+2200 (± 150)	+1670 (± 20) +1140 (± 440)*	+2890 (± 20)
Final Residual Strain after Unloading ($\times 10^{-6}$)	-1230 (± 70)	+2000 (± 130)	+1400 (± 20)	+2200 (± 10)

(*) Average *microscale* data obtained with a $90 \times 90 \mu\text{m}^2$ X-ray beam (the standard deviations are indicated in parentheses). The other strain data was collected with a $2 \times 2 \text{ mm}^2$ X-ray beam (the errors indicated for this data are due to peak fitting).

The thermal residual strains in the matrix exhibit an average of $+2200 \mu\epsilon$ (obtained from the Rietveld analysis of the α -Ti phase). Based on these strain data, the FEM predicts average longitudinal residual stress values of -740 MPa (in fibers) and $+350 \text{ MPa}$ (in the matrix).

The thermal residual strains in the matrix show a higher variation than those in the fibers (Table 1). The 9 matrix locations sampled by the small X-ray beam yielded an average residual strain of $+1140 \mu\epsilon$ with a standard deviation of $440 \mu\epsilon$. Thermal residual strain values ranging from $430 \mu\epsilon$ to $1700 \mu\epsilon$ were measured at these matrix locations. At this point it is important to point out that the matrix grain size ($\sim 29 \mu\text{m}$ [9]) was significant in comparison with the sampling volume used in the microscale measurements. As a result, very few matrix grains (sometimes only one) contributed to the diffracted intensity at a given location. For this reason, the microscale measurements nearly sampled the grain-to-grain strain variations in the matrix.

A possible source of these strain variations is the significant elastic and plastic anisotropy found

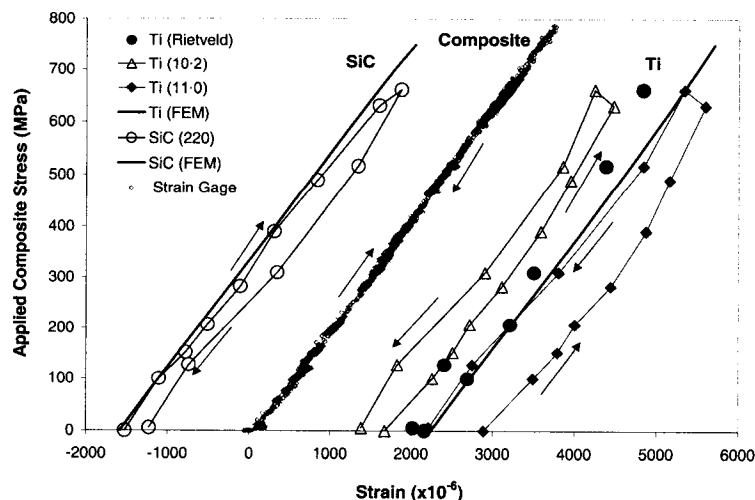


Figure 1. Comparison of experimental data with FEM predictions of applied composite stress vs. average longitudinal strains in the Ti-SiC composite during a loading/unloading cycle. Strain gage values are shown together with lattice strains in the Ti (10-2), Ti (11-0) and SiC (220) reflections obtained from diffraction. A $2 \times 2 \text{ mm}^2$ X-ray beam was used. Thermal residual strains are included (see Table 1).

in the Ti-6Al-4V matrix. This is seen in Table 1 when the *macro* thermal residual strains obtained from different matrix reflections are compared with the Rietveld average. Similar results were also observed by other researchers. For instance, Choo *et al.* [8] obtained $+2600 \mu\epsilon$ in α -Ti from Rietveld analysis. In addition, their plane-specific residual strains are similar to those shown in

Table 1. The residual thermal strain anisotropy in α -Ti is due to anisotropy in its CTE (e.g., the CTE of the basal plane is higher than that of the prism planes) as well as its plastic anisotropy [8]. The latter would manifest itself in terms of variations in susceptibility to plastic deformation during cooling to relieve thermal stresses. As a result, plane-specific residual strains would be relaxed to varying degrees along prism planes in comparison with the basal planes.

Further proof of the consequences of plastic deformation in the matrix was also observed in this study. Single peak fits to the *macro* XRD data showed that, as the composite was loaded up to 500 MPa, the fibers and matrix co-deformed linearly (see Fig. 1). At higher stresses, the fibers began to strain more than the matrix at the same applied stress. This is a clear signal of load transfer to the fibers and implies yielding in the matrix. From FEM, matrix yielding is expected to commence as a thin layer around the fibers. Since X-rays sampled the entire cross-section, matrix yielding was not realized until a significant plastic layer formed. The measured strains then confirm the FEM prediction that “global” yielding will not be apparent until about 600 MPa applied stress (Fig. 1). The matrix yielded around the same stress predicted by the FEM, an *in-situ* yield point of approximately 700 MPa. Note that the strain gage data suggests the composite is linear elastic up to 800 MPa applied stress.

The outcome of matrix yielding is clearly visible in Fig. 1 and Table 1 as changes in the residual strains following unloading. Specifically, new tensile strains (about $+300 \mu\epsilon$) are generated in the fibers and new compressive strains (about $-200 \mu\epsilon$ using the Rietveld analysis) are added to the matrix. The character of the yielding-induced residual strains is typical for a metal matrix composite in which the matrix yields and transfers load to the stiffer fibers [1,6].

Despite the fact that a small change in the “average” matrix residual strains (provided by Rietveld) was observed after the plastic deformation, significant plastic anisotropy was seen in the matrix (Fig. 1 and Table 1). This is expected given the hexagonal crystal structure of α -Ti. Of the two crystal planes exhibited in Fig. 1, (10-2) is closer to the Rietveld average in terms of its susceptibility to plastic deformation. Its effective elastic constant is closer to that given by Rietveld as well—the unloading gradient of (10-2) was measured as 217 GPa versus 221 GPa from Rietveld. In comparison, (11-0) had an unloading gradient of 203 GPa.

In summary, significant elastic and plastic anisotropy exists in the Ti-6Al-4V matrix. This leads to large grain-to-grain strain variations. When microscale strain measurements are performed on a scale comparable to grain size, these strain variations are reflected in the diffraction data from the matrix. Furthermore, the strain data obtained from the fibers at the same scale is also affected by the matrix strain variations.

Conclusions

Using X-ray microdiffraction, the phase specific *in-situ* residual and applied strains in a metal matrix composite were investigated. Due to the CTE mismatch, initial thermal residual stresses of -740 MPa in the fibers and $+350$ MPa in the matrix (on average) exist along fiber axes. In addition, the local residual strain variation was examined showing that the matrix residual strain could vary by as much as 50%. This variation was also reflected in the fiber strains creating locations where the residual compressive stress partially relaxed. Significant relaxation of the residual stress promotes the nucleation of fiber failure under additional stress [10]. Although, using conventional mechanical testing, the global yielding of the Ti-SiC composite was not detected until at least 800 MPa applied stress; XRD strains revealed that local yielding occurred as early as 600 MPa. In the residual stresses and under the applied tensile load, plastic anisotropy was observed in the matrix. It provided a source for the grain-to-grain strain variation in the composite.

Acknowledgments

The authors are grateful to Dr. H. Deve at 3M Corp. for providing the specimens and helpful discussions about the properties of Ti-SiC composites. They also express their gratitude to Dr. I. C. Noyan at IBM Watson Research Center for the use of his stress fixture. This study was supported

by the National Science Foundation (CAREER grant no. DMR-9985264) at Caltech and a Laboratory-Directed Research and Development Project (no. 2000043) at Los Alamos. The work at the Advanced Photon Source was supported by the U.S. Department of Energy, Office of Basic Energy Sciences (contract no. W-31-109-ENG-38).

References

- [1] J. C. Hanan, I. J. Beyerlein, E. Üstündag, G. A. Swift, B. Clausen, D. W. Brown, M. A. M. Bourke, *Adv. in Fracture Research ICF* **10**, Elsevier, UK (2001).
- [2] J. He, I. J. Beyerlein, D. R. Clarke, *J. Mech. Phys. Solids*, **47** (1999), p. 465.
- [3] H. M. Rietveld, *J. Appl. Cryst.*, **2** (1969), p. 65.
- [4] A. C. Larson, R. B. Von Dreele, GSAS-General Structure Analysis System, LAUR 86-748, Los Alamos National Laboratory, (1986).
- [5] P. Rangaswamy, M. B. Prime, M. R. Daymond, M. A. M. Bourke, B. Clausen, H. Choo, N. Jayaraman, *Mater. Sci. Eng.*, **A259** (1999), p. 209.
- [6] P. J. Withers. and A. P. Clarke, *Acta Mater.*, **46**(18) (1998), p. 6585.
- [7] D. B. Gundel and F. E. Wawner, *Comp. Sci. Tech.*, **57**(4) (1997), p. 471.
- [8] H. Choo, P. Rangaswamy and M. A. M. Bourke, *Scripta Mater.*, **42** (2000), p. 175.
- [9] J. C. Hanan, E. Üstündag, D. Dragoi, I. C. Noyan, D. R. Haeffner and P. L. Lee, *Adv. X-Ray Anal.*, **44** (2000), p. 156.
- [10] J. C. Hanan, G. A. Swift, E. Üstündag, I. J. Beyerlein, J. D. Almer, U. Lienert and D. R. Haeffner, submitted to *Metall. Mater. Trans.* (2002).